Received: 30 June 2023 | Revised: 13 September 2023 | Accepted: 14 September 2023

DOI: 10.1002/bit.28562

ARTICLE

BIOTECHNOLOGY AND BIOENGINEERING WILEY

Enhancing the production of recombinant adeno-associated virus in synthetic cell lines through systematic characterization

Min Lu | Zion Lee | Yu-Chieh Lin | Ibrahim Irfanullah | Wen Cai | Wei-Shou Hu

Department of Chemical Engineering and Materials Science, University of Minnesota, Minneapolis, Minnesota, USA

Correspondence
Wei-Shou Hu, 421 Washington Ave SE, Minneapolis, MN 55455-0132 USA.
Email: wshu@umn.edu

Funding information
NSF, Grant/Award Number: DMR-2011401; NNCI, Grant/Award Number: ECCS-2025124

Abstract

Recombinant adeno-associated virus (rAAV) is among the most commonly used in vivo gene delivery vehicles and has seen a number of successes in clinical application. Current manufacturing processes of rAAV employ multiple plasmid transfection or rely on virus infection and face challenges in scale-up. A synthetic biology approach was taken to generate stable cell lines with integrated genetic modules, which produced rAAV upon induction albeit at a low productivity. To identify potential factors that restrained the productivity, we systematically characterized virus production kinetics through targeted quantitative proteomics and various physical assays of viral components. We demonstrated that reducing the excessive expression of gene of interest by its conditional expression greatly increased the productivity of these synthetic cell lines. Further enhancement was gained by optimizing induction profiles and alleviating proteasomal degradation of viral capsid protein by the addition of proteasome inhibitors. Altogether, these enhancements brought the productivity close to traditional multiple plasmid transfection. The rAAV produced had comparable full particle contents as those produced by conventional transient plasmid transfection. The present work exemplified the versatility of our synthetic biology-based viral vector production platform and its potential for plasmid- and virus-free rAAV manufacturing.

KEYWORDS
adeno-associated virus, biomanufacturing, gene therapy, synthetic biology

1 | INTRODUCTION

Recombinant adeno-associated virus (rAAV) is one of the most commonly used delivery vehicles for gene therapy. Its many advantages include effective in vivo gene delivery, long-term persistency, different tissue tropism by various serotypes, and high safety (Samulski & Muzyczka, 2014). Several rAAV-based products, including Luxturna for retinal dystrophy, Zolgensma for spinal muscular atrophy, and Hemgenix for hemophilia B have been approved by the United States Food and Drug Administration in recent years, paving the way for more rAAV-based therapies to come (Herzog et al., 2023; Li & Samulski, 2020). However, a very large dosage of rAAV is required in clinical applications (Mendell et al., 2017), and the manufacturing of large

quantities of rAAV poses a significant challenge. Innovations in rAAV vector manufacturing are called for to create a scalable and robust production platform to meet the demand.

AAV is a small, nonenveloped capsid virus with a single-stranded DNA genome encoding two genes, *rep* and *cap*, flanked by inverted terminal repeats (ITRs) (Sonntag et al., 2010a; Srivastava et al., 1983). AAV as a replication-defective virus, needs the coinfection of a helper virus such as Adenovirus (Ad) to have efficient *rep/cap* gene expression and virus genome replication (Stutika et al., 2016). With alternative splicing and multiple translation initiation sites, both *rep* and *cap* genes generate multiple transcripts and proteins. The large Rep proteins, Rep78 and Rep68, have multiple functions, including DNA binding, ATP-dependent endonuclease, and helicase activities (Im & Muzyczka, 1990) to bind and nick ITRs for AAV genome replication. The small Rep proteins, Rep52 and Rep40, use their helicase activity to encapsidate AAV genomes into pre-formed capsids (King et al., 2001). The *cap* gene encodes VP1, VP2, and VP3 capsid subunits which at a 1:1:10 ratio assemble into the 60-subunit capsid. After translation in the cytoplasm, their translocation into the nucleolus and assembly is facilitated by the assembly-activating protein (AAP) (Sonntag et al., 2010b). Recently, the membrane-associated assembly protein (MAAP) expressed from a novel open reading frame (ORF) in the *cap* gene was found to modulate the secretion of AAV (Elmore et al., 2021; Ogden et al., 2019). Successful AAV genome replication also requires the participation of components from Ad, such as DNA-binding protein (DBP) which increases the processivity of DNA replication (Ward et al., 1998), and E1B55K/E4orf6 complex, which mediates degradation of host cellular proteins such as the MRN complex and p53 (Querido et al., 2001; Schwartz et al., 2007).

To make AAV a gene therapy agent, the *rep* and *cap* genes in the genome are replaced by a gene of interest (GOI) which is to be expressed upon delivery to target cells. The resulting rAAV genome thus lacks the two essential genes for its replication. rAAV is most commonly produced by triple transfection of HEK293 cells with three plasmids, one containing the rAAV genome and two others providing *rep/cap* genes and helper viral genes including *E2A*, *E4*, and *VA RNA* in trans, respectively (Matsushita et al., 1998). Additional Ad helper genes, *E1A* and *E1B*, are already part of the HEK293 genome (Lin et al., 2014). This method produces rAAV readily but is cumbersome in large-scale manufacturing as large quantities of multiple plasmids must first be produced (Srivastava et al., 2021).

Alternative methods of rAAV production use recombinant helper viruses, such as co-infecting Baby Hamster Kidney (BHK) cells with two strains of replication-defective recombinant herpes simplex viruses (rHSV) containing rAAV genome and *rep/cap* genes, respectively (Clément et al., 2009). A similar approach using recombinant Ad also produced rAAV (Merten et al., 2005). The potential of contamination by helper viruses in rAAV products requires additional downstream purification (Penaud-Budloo et al., 2018). To alleviate the concern about residual adenovirus contamination in the product, a tetracycline-enabled self-attenuating Ad was used (Su et al., 2022). Production systems using native *rep/cap* genes present the possibility of generating replication-competent AAV (rcAAV) through homology between the ITR and p5 promoter and through non-homologous recombination (Allen et al., 1997). rAAV was also produced in a baculovirus-based platform by coinfecting insect cells, *Spodoptera frugiperda* (Sf9), with three strains of recombinant baculovirus (rBV) with rAAV genome, *rep* gene, and *cap* gene, respectively (Urabe et al., 2002). Later, the system was streamlined to only two rBVs, one carrying the *rep* and *cap* genes, and the other carrying the rAAV genome (Smith et al., 2009). A safety feature of this system was that *rep* and *cap* genes were separated with opposite transcriptional orientations, and the native viral p5 promoter was replaced by heterologous promoters (Allen et al., 1997; Penaud-Budloo et al., 2018; Wright, 2014) so that rcAAV could not be formed. Another system, Monobac, used a single baculovirus encoding AAV *rep/cap* genes and rAAV genome to produce rAAV8, thus reducing baculovirus DNA contamination in the product (Galibert et al., 2021).

Others have sought to create cell lines, which can be rescued to produce rAAV with or without additional virus infection. By integrating the rAAV vector genome and *rep/cap* genes into HeLa cells, rAAV was produced by infection with Ad (Clark et al., 1995). To eliminate the need for infection of Ad, a HeLa cell line was constructed by integration into its genome an inducible *E1A-E1B* along with rAAV genome, *rep/cap*, *E2*, *E4*, and *VA* RNA genes (Qiao et al., 2002). The cell line was shown to produce rAAV in the early passages but lost productivity gradually over time. The OneBac system used a *rep-cap* expressing Sf9 cell line, which upon infection with an rBV carrying the rAAV genome, produces the rAAV (Mietzsch et al., 2013). A number of improvements were reported to enhance the quality and productivity of the Sf9 system (Mietzsch et al., 2017; Moreno et al., 2022); however, the possible effect of different posttranslational modifications of rAAV produced in Sf9 cells and in human cells needs to be further investigated (Rumachik et al., 2020). A HEK293 cell-based rAAV production platform with inducible *rep*, *cap*, and helper genes was reported to produce rAAV, but the construction of the cell line was not described (Mainwaring et al., 2021).

We have taken a synthetic biology approach to construct HEK293 cell lines which harbor the rAAV genome and genetic modules that can be induced to express necessary replication, helper, and structural components to produce rAAV (Lee et al., 2022). The approach opened a new paradigm of viral vector production through the creation of a stable cell line. However, in those first-generation cell lines, the productivity was low. Here, we report enhancing rAAV productivity in synthetic cell lines through data-driven redesign of genetic modules and tuning of viral gene expression. The method can be readily applied to rAAV of different serotypes with different GOI. Such a stable cell line system will greatly facilitate large-scale manufacturing of rAAV.

2 | MATERIALS AND METHODS

2.1 | Vectors

The rAAV2-GFP genome from pAAV-CAG-GFP (Addgene) was cloned into a Leap-In transposon backbone (ATUM) with a *lacI* repressor gene linked to a puromycin resistance gene driven by a phosphoglycerate kinase promoter, and CAG promoter was replaced with RSV-LacO promoter (Agilent), yielding the inducible rAAV genome module (GM; Figure 1a). The construction of the replication module (RM) and packaging module (PM) was previously described (Lee et al., 2022). Modification of RM was made by replacing the GeneSwitch promoter with a TetON promoter and removing the GeneSwitch transactivator gene, yielding the new RM (Figure 1a). pAAV-CAG-GFP (Addgene), pAAV-RC2 (Cell Biolabs), and pHelper vectors (Cell Biolabs) were used for triple transfection.

2.2 | Generation of rAAV producer cell lines

HEK293 cells (Cell Biolabs) were cultured in Dulbecco's Modified Eagle Medium (DMEM; Gibco) supplemented with 10% fetal bovine Serum (Gibco) and 1X antibiotic-antimycotic (Gibco). GX stable cell lines were generated by cotransfection of three transposon modules with Leap-In Transposase® mRNA (ATUM) followed by selection, single-cell cloning, and productivity screening. The workflow is in reference to the previous report and is fully described in Supporting Information: Figure S1C–F (Lee et al., 2022; Lee et al., 2023).

2.3 | Cell culture and rAAV vector production

For rAAV production using GX cell lines, cells were seeded at 3.75×10^5 cells per well in 6-well plates or 7.5×10^4 cells per well in 24-well plates. After 24 h, media were replaced with induction media containing 10 µg/mL of doxycycline and 90 µg/mL of cumate (Sigma Aldrich) unless noted otherwise. For proteasome inhibitor experiments, 1 µM of MG132 (Invivogen) was added to GX cells at 24 h postinduction (hpi), and cells were incubated with inhibitors for 24 h before media replacement unless noted otherwise. Cells were harvested at 72 hpi. Extraction methods and quantitative polymerase chain reaction (qPCR) assays of intracellular DNA and RNA were previously described (Lee et al., 2022).

2.4 | rAAV preparation and characterization

Preparation of benzonase-treated rAAV crude lysate and titration of encapsidation vector genome (VG) by qPCR, capsids by enzyme-linked immunosorbent assay (ELISA), and transducing units by RM4 assay cells were previously described (Lee et al., 2022). Total intracellular virus genome (TG) copies, including free virus genomes and encapsidated VGs were measured by qPCR using total intracellular DNA. The full particle content was obtained by dividing the VG by the capsid titer (Grimm et al., 1999).

2.5 | Targeted quantitative proteomics

Sample processing, parameters used for data acquisition by mass spectrometry with parallel reaction monitoring (PRM) method, and data analysis were described previously (Lee et al., 2022). Four new heavy isotope-labeled peptides of VP1, GFP, Rep, and beta-actin proteins were synthesized (Biosynth), and a full list of peptide standards is shown in Supporting Information: Table S1.

2.6 | Transmission electron microscopy and Cryo-EM

rAAV crude lysate was produced in multiple 150 mm dishes, and then purified using POROS CaptureSelect AAVX (Thermo Fisher Scientific) affinity chromatography. rAAV containing cell lysate was loaded, and the column was subsequently washed with 1× TD buffer (5.3 mM KCl, 137 mM NaCl, 10 mM Na_2HPO_4, 1.8 mM KH_2PO_4, and 1 mM $MgCl_2$) (Mietzsch et al., 2020). The adsorbed rAAV was eluted with 0.1 M glycine-HCl (pH 2.6). The rAAV eluate was immediately neutralized with 1 M Tris-HCl (pH 10). For negative-staining TEM, 5 µL of the purified AAV sample was applied to a glow-discharged 400 mesh ultra-thin carbon grid (Electron Microscopy Sciences) and stained by 2% uranyl formate solution (w/v), then blotted dry. For cryo-EM, 3 µL of sample was applied to a glow-discharged R2/1 200 mesh Quantifoil TEM grid (Ted Pella). The blotted dry grid was plunged into liquid ethane, then transferred at the liquid nitrogen temperature to an FEI Tecnai 300 kV field emission gun TEM (Thermo Fisher Scientific). The images were recorded on a Gatan 4k slow scan CCD camera or a Gatan Summit K2 direct electron detector camera (Gatan).

3 | RESULTS

3.1 | Controlled gene expression of GOI increased productivity

We had previously established Pf3 cell line, which synthesized rAAV expressing green fluorescence protein (GFP) as GOI upon induction (Lee et al., 2022). In Pf3 cells, the expression of GFP was driven by a strong constitutive CAG promoter. Its *cap* was encoded by a single intron-less transcript with altered translation initiation, which has been reported to give a more favorable ratio of VP1:VP2:VP3 and denoted as VP123 (Urabe et al., 2002). We used transcriptomic and proteomic analysis to probe potential limiting factors whose relaxation could lead to enhanced productivity. Pf3 had a transcript level of GFP several times of GAPDH even under uninduced

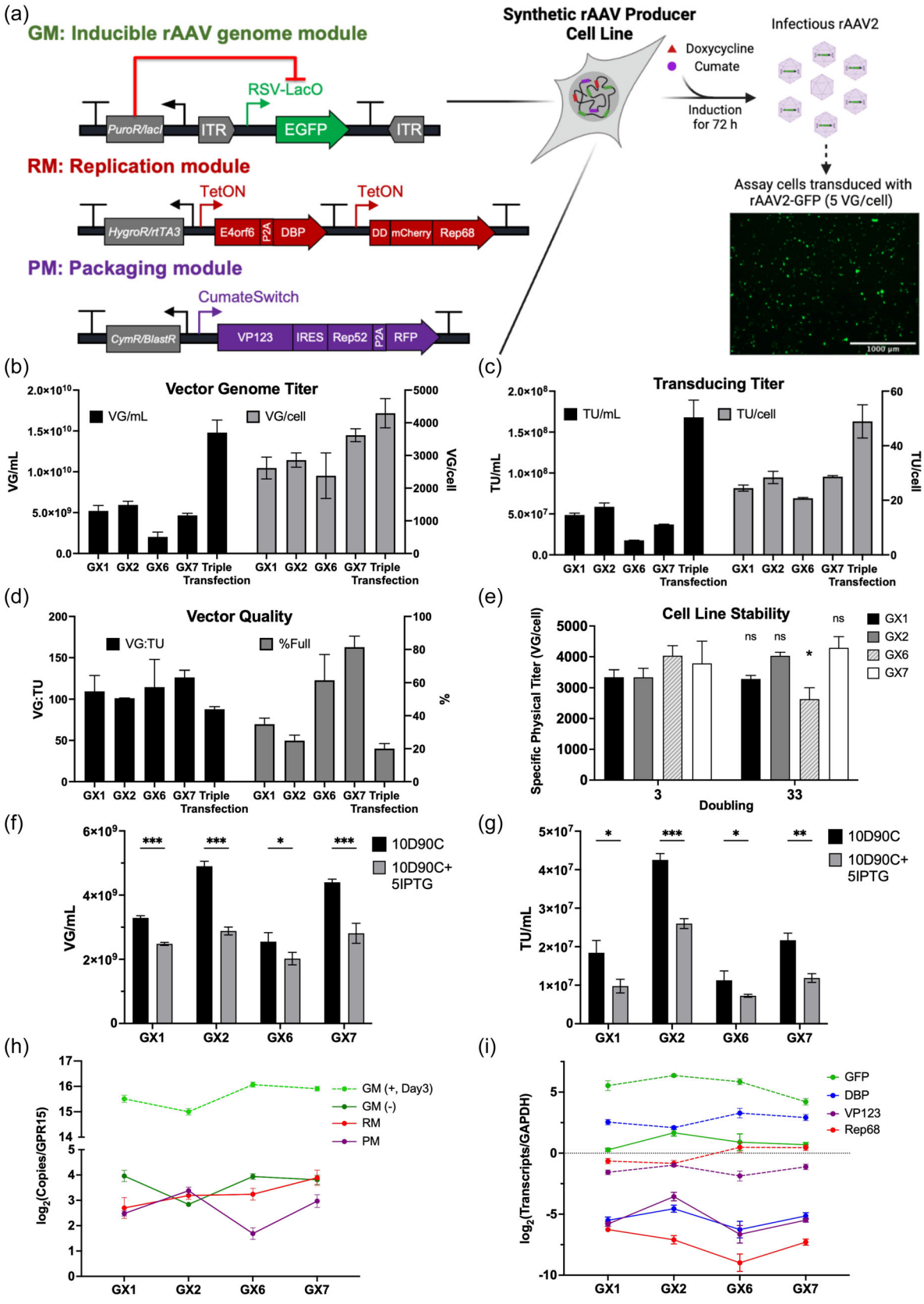

FIGURE 1 (See caption on next page).

conditions (Supporting Information: Figure S1A). GFP transcript level increased almost 20-fold upon induction. After viral genome amplification, GFP transcript accounted for 93% of total viral transcripts or 17% of total cellular mRNAs. In comparison, VP123 transcript constituted only 1.64% of viral RNAs or 0.3% of total mRNAs. At the protein level, GFP was also much higher than other viral proteins (Supporting Information: Figure S1B). Based on the results, we hypothesized that such excessive and wasteful expression of GOI diverted resources, which could have been used for transcription and/or translation of viral genome and proteins and contributed to the low virus productivity. We postulated that minimizing GOI expression in producing cells would increase rAAV production.

We replaced the CAG promoter for GFP in the Genome module (GM) with the Rous sarcoma virus (RSV) promoter controlled by lac operators and repressors (Figure 1a) (Wyborski & Short, 1991). The IPTG-inducible lac repressor gene, *lacI*, was placed upstream of the AAV ITR and linked to a puromycin resistance gene via a 2A self-cleaving peptide. Under uninduced conditions, *lacI* is expressed to suppress GFP expression. The replicated and encapsidated genome does not have the *lacI* gene. Upon transducing into a *lacI*-free recipient cell, GFP can be expressed. Additionally, we made a modification to the replication module (RM). The TetON inducible promoter was used to control both Rep68 and helper genes to reduce the size of the RM, eliminating the need of the transactivator for a second inducible promoter. HEK293 cells were transfected with the inducible GM, RM, packaging module (PM), and Leap-In Transposase® mRNA. Cells were selected with puromycin, hygromycin, and blasticidin for 2 weeks followed by single-cell cloning. Over 60 clones were screened for high rAAV titer using RM4 assay cells upon induction with 10 μg/mL of doxycycline (Dox) and 90 μg/mL of cumate (10D90C) (Supporting Information: Figure S1C–E) (Lee et al., 2023). The top four rAAV-producing clones (GX1, GX2, GX6, and GX7) were isolated, expanded, and further characterized.

GX1, 2, and 7 produced around 5×10^9 encapsidated vector genomes (VG) per mL, and all four clones produced roughly 3000 VG per cell (Figure 1b) upon induction by Dox and cumate. A parallel triple transfection using the traditional pAAV-GFP, pAAV-RC2, and pHelper vectors yielded a somewhat higher titer. The transducing titer (assayed using RM4 assay cells and called transducing units [TU]) (Lee et al., 2023) largely followed the trend of vector genome titer (i.e., VG titer) for all four clones (Figure 1c). The VG:TU ratio was around 100:1, and the full particle content estimated by VG to capsid ratio was from approximately 25% to 80% (Figure 1d). In general, the quality of viral vectors produced using the four clones, in terms of VG:TU and full particle content, was similar to or better than triple transfection. Three out of four clones kept the same productivity after 30 doublings (Figure 1e). We evaluated the effect of inducing GOI expression on the rAAV productivity. The *rep*, helper and *cap* genes were induced with or without IPTG induction of GFP expression. With 5 mM of IPTG, producer cells became much greener, and both VG and TU titers markedly decreased in all four clones (Figure 1f,g and Supporting Information: S1F–I). The result indicated that a high level of GOI expression impeded rAAV production.

The number of copies of each module integrated into the host cell genome, that of amplified viral genome after induction for 72 h, and the transcript level of viral genes were determined via qPCR. The three modules were integrated into the genome in somewhat different numbers for each clone (Figure 1h). All four clones had four to eight times more GM integrated than the previously established Pf3 cell line (Lee et al., 2022). Induction at 10D90C caused rAAV genome to replicate to more than 10^5 copies per cell. Although the number of cell clones was small, there appears to be a correlation between copy number of integrated GM to total number of amplified genomes. The genes encoded in RM and PM modules had low levels of leaky expression, but GFP in GM was expressed slightly higher than GAPDH (Figure 1i). Upon induction, all viral transcripts became highly expressed. GFP reached a very high level of expression even though its promoter was uninduced because of rAAV genome amplification that could have exhausted the lacI repressor protein.

FIGURE 1 Construction and characterization of GX rAAV2 producer cell lines. (a) Gene modules. Symbols: CymR: the Cym Repressor; DD: the destabilization domain; LacO: the lactose (lac) operator; RSV: the Rous sarcoma virus promoter; rtTA3: the reverse Tet transactivator gene. (b) Encapsidated vector genome (VG) titers. (c) Transducing unit (TU) titers. (d) The ratio of VG to TU and VG to capsid as vector quality parameters. (e) Specific rAAV titer in VG/cell at 3 and 33 population doublings. (f and g) VG and TU titers with or without induction of GOI expression by addition of 5 mM of IPTG. (h) Intracellular copy numbers of GM, RM, and PM before induction (solid lines) and GM after induction with Dox and cumate for 72 h (+, dash line). (i) Transcript level of viral genes relative to GAPDH before induction (solid lines) and after Dox and cumate induction for 72 h (dash line). rAAV production using GX cell lines was carried out by inducing GX cell lines with 10 μg/mL of Dox and 90 μg/mL of cumate (10D90C) for 72 h. For (b–d), triple plasmid transfection of HEK293 cells with pAAV-CAG-GFP, pAAV2-RC, and pHelper was included for comparison with GX cell lines. Encapsidated VG titers were measured by qPCR, TU titers by image analysis using RM4 assay cells, and capsid titers by ELISA. For (b–g), data represent mean and standard deviation of three independent replicates. For (h) and (i), data represent mean and standard deviation of triplicate qPCR wells. ns: $p > 0.05$, $^*p < 0.05$, $^{**}p < 0.01$, $^{***}p < 0.001$ as determined by an unpaired, two-tailed, two-sample *t*-test. Multiple-comparisons *t*-test was assessed by using a false discovery rate (FDR) of 0.05. ELISA, enzyme-linked immunosorbent assay; GFP, green fluorescence protein; GM, genome module; GOI, gene of interest; IPTG, isopropyl β-D-1-thiogalactopyranoside; PM, packaging module; qPCR, quantitative polymerase chain reaction; rAAV, recombinant adeno-associated virus; RM, replication module.

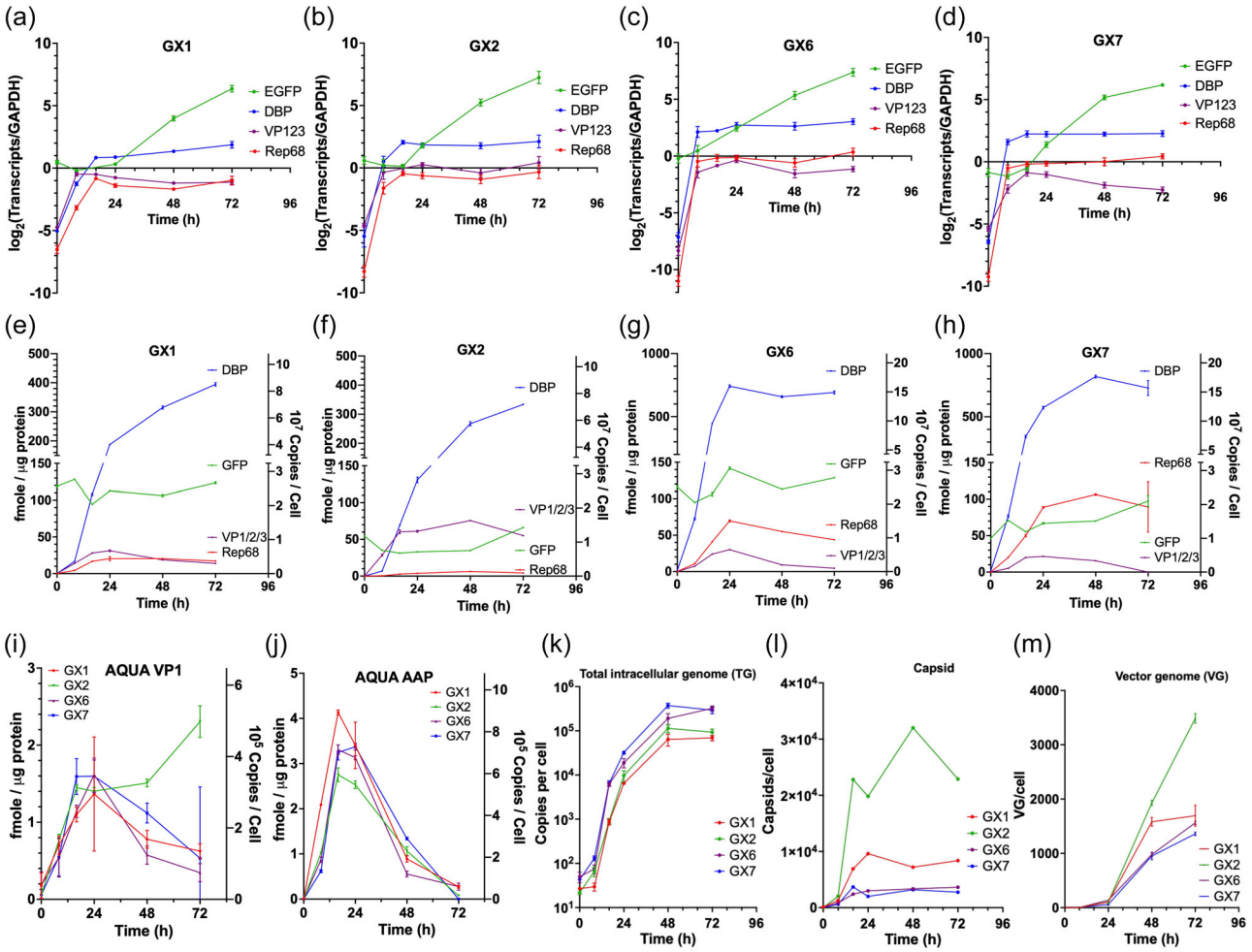

FIGURE 2 Kinetic profiles of viral transcripts and proteins, total intracellular virus genome, assembled capsids, and vector genome in GX cell lines upon induction. (a–d) Transcript level of viral genes relative to GAPDH. (e–j) Absolute quantification (AQUA) of viral proteins measured by mass spectrometry with the parallel reaction monitoring (PRM) method. Protein copies per cell were calculated based on the assumption that total protein from one HEK293 cell is 360 pg. (k) Total intracellular virus genome copies per cell. (l) Assembled capsids per cell. (m) Encapsidated VG per cell. Samples were prepared by inducing GX cell lines with 10D90C. For (a–d, k, and m), data represent mean and standard deviation of triplicate qPCR wells. For (e–j), data represent mean and standard deviation calculated from light to heavy peak area ratios of top three fragment ions in ion chromatograms multiplied by the concentration of peptide standards. For (l), data represent the mean of duplicate ELISA wells. ELISA, enzyme-linked immunosorbent assay; qPCR, quantitative polymerase chain reaction; VG, vector genome.

3.2 | Dynamics of viral gene expression and virus assembly

We characterized the time-course profiles of various viral components after induction. The transcript level of three viral genes, Rep68 and DBP in RM and VP123 in PM, increased rapidly upon induction with Dox and cumate and reached close to GAPDH level by 8 h before leveling off around 16 h in all four cell lines (Figure 2a–d). Consistent with the results of Figure 1i, DBP was the most highly expressed viral gene in all four cell lines. The transcript levels of Rep68 and the VP123 were several folds lower but still at high levels similar to GAPDH. GFP transcript followed different dynamics to the viral genes. It started from a high leaky expression level and increased as the viral genome replicated despite the absence of inducer IPTG.

Targeted quantitative proteomics was performed on heavy isotope-labeled peptide spiked samples to quantify key proteins. By abundance level they fell into two broad groups: Rep68, DBP, VP1/2/3 (quantified using a peptide common to VP1, VP2, and VP3), and GFP in the order of 100 fmol/µg protein (Figure 2e–h), while VP1 (quantified using a peptide unique to VP1) and AAP in approximately the level of 5 fmol/µg protein (Figure 2i–j). The rise of viral proteins lagged somewhat from the corresponding transcript; the initial fast rise transited to a slower increase around 24 h. The relative abundance level and dynamics of different proteins followed similar trends in different clones. The most abundant protein was DBP which had more than 10^7 copies per cell. Notably, VP1 and AAP proteins decreased sharply after peaking around 24 h, along with a similar but less drastic decrease of VP1/2/3. The decrease of VP proteins was also shown in western blot analysis (Supporting Information:

Figure S2). DBP was the only detectable viral protein in uninduced conditions, which had around 5×10^4 copies per cell. A housekeeping protein, beta-actin, had 10^7 copies per cell and remained steady across different conditions (data not shown).

Total intracellular virus genomes, including those encapsidated and free ones, reached approximately 10^4 copies at 24 h and increased to around 10^5 copies by 48 h (Figure 2k). From 10^6–10^7 copies per cell of VP1/2/3 protein, about 10^3–10^4 of capsids were assembled at 24 h (Figure 2l). However, the vast majority (> 90%) of genome copies and most encapsidated genomes (VGs) were formed after 24 h (Figure 2m). Each capsid constitutes 60 VP subunits, hence approximately 3%–10% of VP1/2/3 proteins were incorporated into capsids (Supporting Information: Figure S3). The data also suggested that capsid assembly initiated early while VP1/2/3 level was still some way from its peak level around 24 h. Compared with the dynamics of other viral components, genome packaging into capsid was a slow process (Figure 2m). Genome encapsidation started early but the rate was slow until total genome copies reached about 10^4–10^5 copies per cell. Only a very small portion of total genomes (0.3%–3%) were encapsidated (Supporting Information: Figure S3). The data suggested that genome packaging is a potential limiting factor.

3.3 | Cell line-dependent optimal induction profile for high productivity

The induction condition used in the preceding experiments was for maximum expression of target genes, which might not be most favorable for rAAV production. A premise of our synthetic biology approach was that the expression profile of viral genes could be modulated by different induction profiles to enhance productivity and product quality. Multiplex screening of the concentration and time profile of Dox and cumate was set up for rAAV production using all four cell lines (Supporting Information: Figure S4A–D). For GX1 and GX2, the initial induction condition (10D90C) gave a good titer, while for GX6 and GX7, a better titer was obtained by reducing the Dox level, removing Dox at 8 h post-induction (hpi), or delaying addition of Dox. The results show the benefit of a tunable induction system on enhancing the rAAV productivity.

The two new induction conditions, reducing Dox from 10 μg/mL to 0.5 μg/mL (0.5D90C) and removing the 10 μg/mL of Dox at 8 hpi (10D90C-8h) were further compared to the original condition of 10D90C in GX6 and GX7. The results confirmed that 0.5D90C and 10D90C-8h gave higher VG, capsid, and TU titers on both a volumetric basis (Figure 3a,b,g,h) and per cell basis (Supporting Information: Figure S4E,F,J,K). Further characterization was performed on the dynamics of viral gene products under these induction conditions. Consistently, induction with 0.5D90C or 10D90C-8h gave higher levels of assembled capsids, VG, and TU than induction with 10D90C (Figure 3c–e,i–k). However, the total intracellular genome was not markedly different among different induction conditions (Figure 3f,l). At the transcript level, expression of Rep68 and DBP decreased greatly with a lower level or removal of Dox as expected (Figure 3m,n,p,q). Since the induction concentration of cumate was the same in all three conditions, VP123 transcript level was similar (Figure 3o,r). Nevertheless, the levels of assembled capsid were higher with lower level or removal of Dox (Figure 3c,i), so was the level of VP1/2/3 proteins in the western blots and immunofluorescence intensity measured by flow cytometry (Figure S4O–Q) suggesting that VP expression might be affected by post-transcriptional regulation.

The kinetic profiles of 0.5D90C and 10D90C-8h were largely similar for both GX6 and GX7. Practically, removing Dox would require the replacement of medium and is difficult to implement in manufacturing. In the following experiments 0.5D90C was adopted for GX6 and GX7.

3.4 | Inhibition of proteasomal degradation increased productivity in synthetic cells

A striking observation on the dynamic behavior of viral proteins through targeted proteomics was the decline of VP1/2/3 and AAP after reaching peak values around 24 h (Figure 2e–j). We postulated that the decrease was caused by proteolytic degradation. In a screening experiment, we tested four proteasome inhibitors on their effect on the infectious rAAV titer under different conditions on the four GX cell lines. An inhibitor was added to cultures at 24 h after induction under optimal induction conditions and incubated for 2, 6, or 24 h before being removed for the remainder of the 72 h. Among the four inhibitors tested, MG132 had a consistent enhancing effect on TU titer using all four cell lines tested (Supporting Information: Figure S5A–P). Two conditions, MG132 (10 μM, 6 h) and MG132 (1 μM, 24 h) were further evaluated and both showed enhancing effect on the rAAV productivity as compared to the case of without MG132. For GX2 and GX6, both conditions had a similar enhancing effect, but for GX1 and GX7, a higher titer was obtained with MG132 (1 μM, 24 h) (Supporting Information: Figure S5Q). In subsequent studies, the MG132 at 1 μM with incubation for 24 h was used for all cell lines.

Targeted proteomics quantification on the cell samples subjected to induction and with or without MG132 (1 μM, 24 h) showed significant increase of VP1/2/3, VP1, and AAP proteins with MG132 for all four cell lines (Figure 4a–c). Since Rep68 was tagged with a destabilization domain, Rep68 abundance also increased by inhibition of proteasomal degradation (Figure 4d). In comparison, the abundance levels of viral protein DBP and viral genome encoded GFP did not increase upon inhibition of proteasome (Figure 4e,f). The effect on viral protein abundance was further verified by immunofluorescence intensity measured by flow cytometry (Supporting Information: Figure S6A–H). With the optimal induction condition and the treatment of MG132, GX2 clones can produce more than 10^4 VG and over 10^5 capsids per cell (Figure 4g,h).

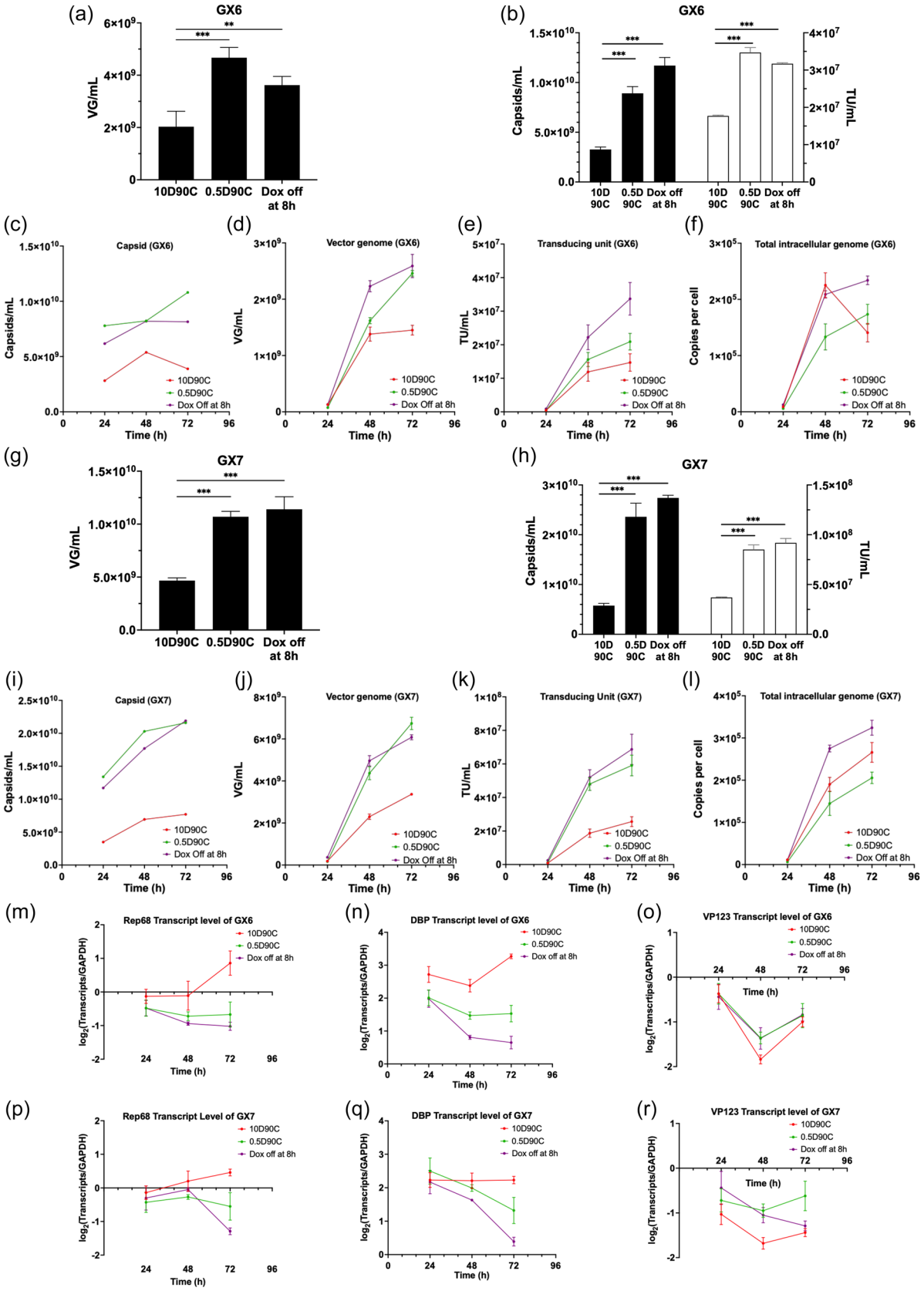

FIGURE 3 (See caption on next page).

3.5 | Full particle content of rAAV produced

The full particle content produced under optimal induction conditions with or without MG132 was determined by taking the ratio of VG to capsids. While total viral particles increased with MG132 treatment, there was a concurrent increase of empty capsids and hence a marginal decrease in the full particle ratio (Figure 5a). Since the full particle content estimated from qPCR and ELISA data had large variations, negative-staining transmission electron microscopy (TEM) and Cryo-EM were used to examine the particle morphology and quantify genome-containing rAAV directly (Subramanian et al., 2019) using samples prepared in two higher producers GX2 and GX7 because of the large quantity of viral particles required for the assay (Supporting Information: Figure S7A–H). Viral particles produced using GX2 and GX7 were 24% and 56% full, respectively, without MG132. Upon MG132 treatment, it remained at a similar level (26%) for GX2 and dropped moderately (42%) in GX7 (Figure 5b).

4 | DISCUSSION

The design of our synthetic cell lines for rAAV production had two key features: the integration of only minimal essential viral elements into the host cell genome and replacing native viral transcription regulation elements with inducible promoters whose expression can be tuned through exogenous chemical signals. In the current study, we reduced wasteful expression of GOI, isolated new clones with a higher copy number of genetic modules, optimized induction profile, and minimized proteasomal degradation of capsid proteins to further advance the productivity. Similar impediment of rAAV production by overexpression of the GOI in transient triple transfection was reported before (Strobel et al., 2015). Using an inducible promoter for GOI, the high-producing GX cell lines isolated indeed had higher numbers of copies of GM integrated into the host genome than the previous Pf cell lines. After induction and genome amplification, the transcript level was still rather high. With our proof-of-concept design of GM, viral genome replication amplified only ITR-flanked regions, but not the *lacI* repressor gene outside the ITR. Hence, after viral genome amplification, the vastly large number of LacO would quickly exhaust LacI repressor proteins and lead to an increased transcript level of GOI. Further suppression of GOI, for example, by using tightly regulated tissue-specific promoters that have been successfully employed in rAAV targeting different tissues such as muscle (Wang et al., 2008), central neuron system (Tenenbaum et al., 2004), heart and liver (Chen et al., 2013) for GOI expression, may further enhance the productivity. We compared common features of four GX lines and compared to those of Pf lines to glean possible features that might contribute to higher productivity (Lee et al., 2022). All four GX cell lines had more copies of GM and RM than Pf lines. Upon induction and genome amplification, the difference in total intracellular virus genome between GX and Pf lines widened to more than 10–200-fold. This might have contributed to the higher VG titer and vector quality in GX cells. Some common patterns in transcript level of viral genes were seen. DBP transcript and protein levels were very high in all four cell lines. Rep68 and VP123 transcript and protein levels were several-fold lower than DBP, and VP1 and AAP had the lowest levels. However, there was a noticeable difference in Rep68 and VP1/2/3 protein levels among clones. GX2 had somewhat higher VP123 transcript and VP1/2/3 protein levels compared to other cell lines. However, with many variables, including genome replication, capsid assembly, and genome packaging in the production of rAAV, it is hard to assess how much the higher VP protein level contributed to the higher productivity of GX2. Although GX cells had more rAAV genome copies than Pf3, GFP protein was lower as attributed to the use of an inducible promoter for GFP.

Using assay cell line RM4, we surveyed rAAV productivity under different combinations of inducer dose and time profile. While higher levels of Dox induction gave higher rAAV titers in GX1 and GX2, reduced Dox induction increased the productivity in GX6 and GX7. With 10D, GX6 and GX7 cell lines expressed somewhat higher levels of Rep68 transcript and markedly higher levels of Rep68 protein than GX1 and GX2 (Figure 2a–h). The observed enhancing effect on rAAV titer in GX6 and GX7 at reduced expression of Rep68 by using a lower Dox or its removal at 8 hpi may reflect a negative influence of high Rep level on rAAV titer. This was consistent with the report that large Rep proteins inhibited translation and elicited apoptosis (Schmidt et al., 2000; Trempe & Carter, 1988).

Our targeted proteomic study revealed possible degradation of AAP and VP1/2/3 proteins after reaching their peak values in all four GX cell lines (Figure 2e–j). AAP facilitates cotransport of VP proteins to the nucleoli and promotes VP protein stability and capsid assembly by oligomerization (Maurer et al., 2018; Sonntag et al., 2010b). Without AAP, VP proteins are subject to degradation through several pathways, including proteasomal degradation in the unfolded protein response (UPR) as part of

FIGURE 3 Induction conditions affected rAAV production by GX6 and GX7 cell lines. (a–f, m–o) For GX6, (g–l, p–r) for GX7 cell line. (a, g) VG, (b, h) capsid and TU titers upon induction with 10D90C for 72 h, 0.5D90C for 72 h, or 10D90C for 8 h, and then with Dox removed for the remainder of 72 h. (c–f, i–l) Kinetic profiles of capsids, total intracellular virus genome, VG, and TU under three induction conditions. (m–o, p–r) Relative transcript levels of viral genes. For a, b, g, and h, data represent mean and standard deviation of three independent replicates. For (c) and (i), data represent mean of duplicate ELISA wells. For (d, e, j, k, and m–r), data represent mean and standard deviation of triplicate qPCR wells. For (f and l), data represent mean and standard deviation of GFP-positive cell counts from 12 images. $^{*}p < 0.05$, $^{**}p < 0.01$, $^{***}p < 0.001$ as determined by a one-way analysis of variance (ANOVA) multiple-comparisons test. ELISA, enzyme-linked immunosorbent assay; GFP, green fluorescence protein; rAAV, recombinant adeno-associated virus; qPCR, quantitative polymerase chain reaction; TU, transducing unit; VG, vector genome.

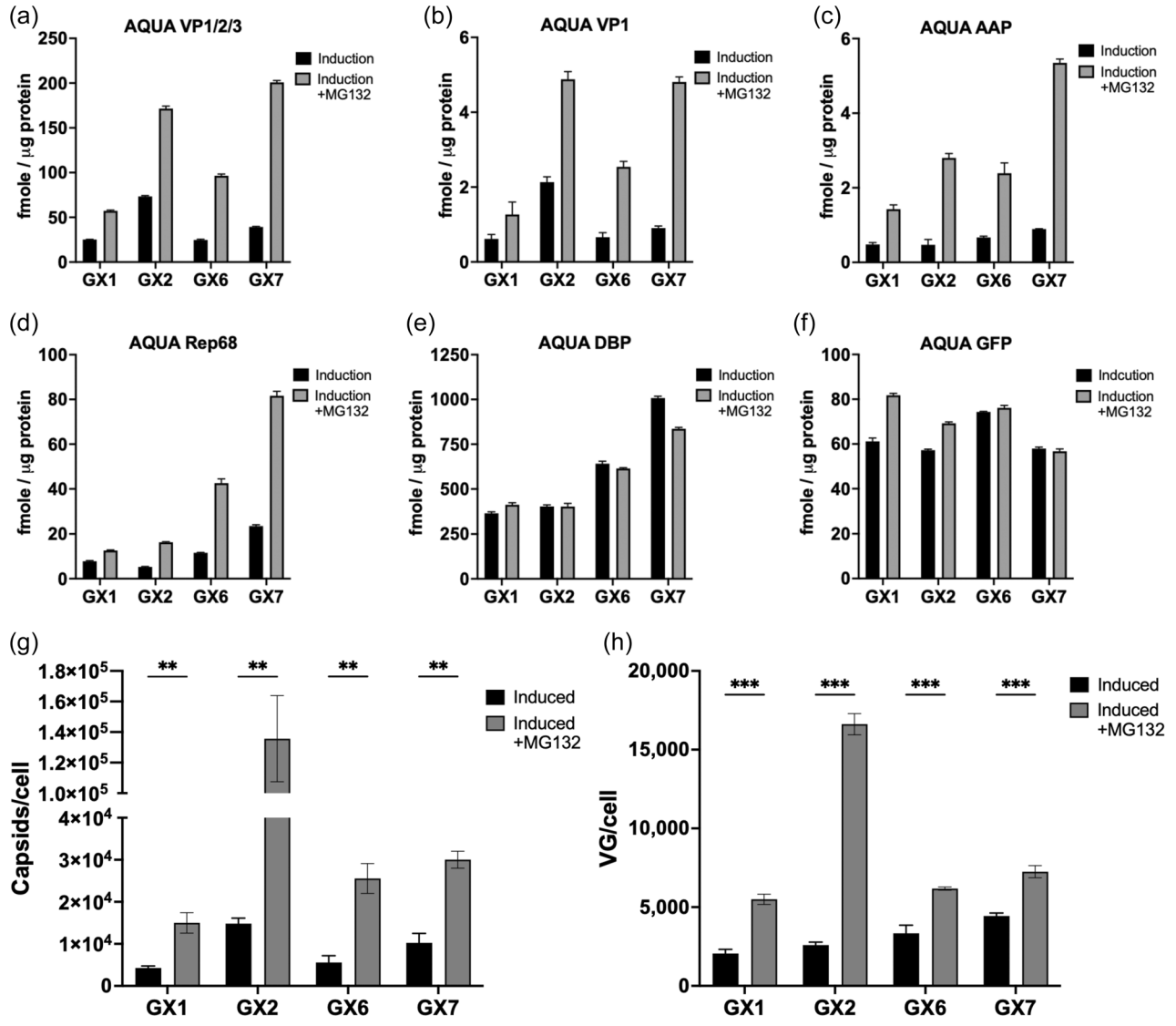

FIGURE 4 Treatment of proteasome inhibitor MG132 increased viral protein abundance and rAAV titers. AQUA of (a) VP1/2/3, (b) VP1, (c) AAP, (d) Rep68, (e) DBP, and (f) GFP. (g) Capsids and (h) VG per cell produced in GX cell lines at 72 hpi with or without MG132. GX1 and GX2 were induced with 10D90C, and GX6 and GX7 were induced with 0.5D90C. Proteasome inhibitor, 1 µM of MG132, was added at 24 hpi for 24 h (MG132, 1 µM, 24 h) before being removed by medium replenishment with fresh induction media. For (a–f), data represent mean and standard deviation calculated from light to heavy peak area ratios of top three fragment ions in ion chromatograms multiplied by the concentration of peptide standards. For (h) and (i), data represent mean and standard deviation of three independent replicates. $^{*}p < 0.05$, $^{**}p < 0.01$, $^{***}p < 0.001$ as determined by an unpaired, two-tailed, two-sample *t*-test. Multiple-comparisons *t*-test was assessed by using an FDR of 0.05. AAP, assembly-activating protein; AQUA, absolute quantification; DBP, DNA binding protein; FDR, false discovery rate; GFP, green fluorescence protein; VG, vector genome.

host cell response to virus infection (Balakrishnan et al., 2013; Prasad & Greber, 2021). Adding a proteasome inhibitor in rAAV transduction has been shown to have an enhancing effect on transgene expression (Jennings et al., 2005; Mitchell & Samulski, 2013). Inhibiting proteasome-mediated degradation during rAAV production led to a higher level of AAV2 capsid proteins and boosted rAAV production. This enhancing effect of rAAV productivity was attainable with a high level of MG132 for a shorter period or by using a low MG132 concentration throughout the induction (Supporting Information: Figures S5Q and S8). The titer-enhancing effect of MG132 provided additional evidence of the role of host cell-initiated degradation in rAAV production.

With enhanced induction conditions and MG132 treatment, the productivity in terms of VG was approaching that of traditional triple transfection. For future manufacturing, one anticipates that the host cells will be suspension-growth adapted to allow for high-density cultures. The use of a chemical inhibitor in manufacturing may not be desirable. One may consider the possibility of knocking out the responsible protease genes.

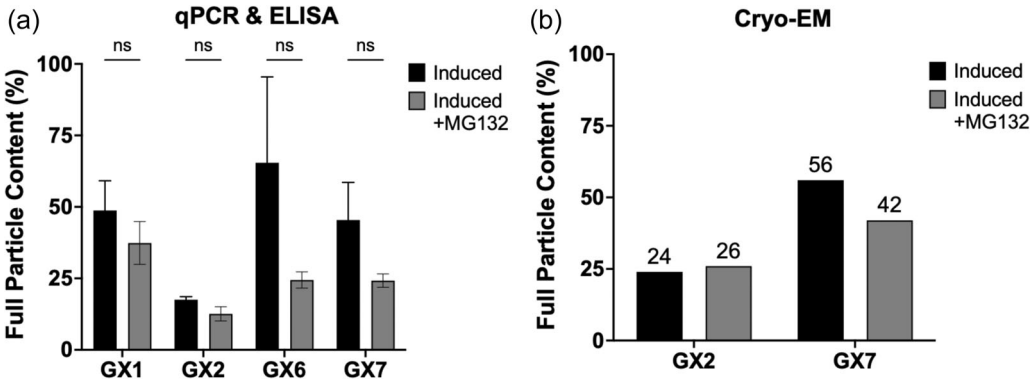

FIGURE 5 Full particle contents produced using GX cell lines under optimal induction conditions with or without MG132 treatment. (a) Full particle content (%) determined by taking the ratio of VG to capsids measured by qPCR and ELISA, respectively. (b) Full particle content (%) determined by Cryo-EM analysis. For (a), data represent mean and standard deviation of three independent replicates. For (b), data represent ratio of full to total particles counted by enumerating particles in multiple Cryo-EM images. ns: $p > 0.05$, as determined by an unpaired, two-tailed, two-sample *t*-test. Multiple-comparisons t-test was assessed by using an FDR of 0.05. Cryo-EM, Cryo-electron microscopy; ELISA, enzyme-linked immunosorbent assay; FDR, false discovery rate; qPCR, quantitative polymerase chain reaction; VG, vector genome.

The full particle content ranged from 25% to over 50%. The value was comparable to or higher than the 30% reported in the literature (Penaud-Budloo et al., 2018). VG:TU ratio is often used as an estimate of rAAV infectivity. Its value can be highly variable between production methods or even preparation lots (François et al., 2018; Mohiuddin et al., 2005). rAAV produced from GX cells across different batches of production had VG:TU about 100, a value comparable to prior reports (Zeltner et al., 2010). While the number of cell lines and rAAV production kinetic studies is still small, a general trend seems to emerge. Increasing the VP1/2/3 protein level results in higher capsid titers as well as VG titers. However, their increase is not proportionate; instead, the capsid titer increases more than the VG titer, leading to a drop in full particle content. An optimal production condition will need to consider both VG titer and full particle content.

We had previously reported proof-of-concept rAAV-producing cell lines created using a synthetic biology approach by employing only essential gene sets for rAAV synthesis and placing them under inducible promoter control (Lee et al., 2022). Here we report our success in further enhancing productivity through cell engineering and optimization of gene expression dynamics and culture conditions. The productivity of the GX cell lines approaches that of commonly used triple plasmid transient transfection. Also, only a tiny portion of the total genome encapsidated, thus one may speculate that the productivity can possibly be enhanced by the higher expression of *cap* genes and increasing the efficiency of viral genome packaging into capsids. Further exploration of helper viral components such as Ad noncoding VA RNA, which inhibits PKR-mediated antiviral response (Vachon & Conn, 2016) and other Ad E4 proteins (e.g., E4orf3 and E4orf6/7) (Huang & Hearing, 1989; Soriano et al., 2019) which modulate host responses along with tempering of host cell responses to rAAV replication may have much enhancing effect on the productivity. With further enhancement, the use of stable cell lines for rAAV manufacturing may become a reality.

AUTHOR CONTRIBUTIONS

Min Lu, Zion Lee, and Wei-Shou Hu conceived and designed the study. Min Lu, Yu-Chieh Lin, Ibrahim Irfanullah, and Wen Cai performed experiments and analyzed data. All authors contributed to manuscript preparation. Wei-Shou Hu supervised the study.

ACKNOWLEDGMENTS

The authors would like to acknowledge the Minnesota Supercomputing Institute (MSI) at the University of Minnesota for providing computational resources for RNA-seq data analysis and the Center for Metabolomics and Proteomics (CMSP) at the University of Minnesota for proteomic analysis. TEM and Cryo-EM was carried out in the Characterization Facility at University of Minnesota, which received partial support from the NSF through the MRSEC (award number DMR-2011401) and the NNCI (award number ECCS-2025124) programs. The Leap-In transposon plasmid backbone and Transposase® mRNA were kindly provided by ATUM. Figure 1a and Supporting Information: S1C and graphic abstract were created with BioRender.com.

CONFLICTS OF INTEREST STATEMENT

The authors declare that there is no conflict of interest.

DATA AVAILABILITY STATEMENT

The data that support the findings of this study are available from the corresponding author upon reasonable request.

ORCID

Zion Lee http://orcid.org/0000-0002-6869-4198
Wei-Shou Hu http://orcid.org/0000-0001-7739-8692

REFERENCES

Allen, J. M., Debelak, D. J., Reynolds, T. C., & Miller, A. D. (1997). Identification and elimination of replication-competent adeno-associated virus (AAV) that can arise by nonhomologous recombination during AAV vector production. *Journal of Virology*, *71*(9), 6816–6822. https://doi.org/10.1128/jvi.71.9.6816-6822.1997

Balakrishnan, B., Sen, D., Hareendran, S., Roshini, V., David, S., Srivastava, A., & Jayandharan, G. R. (2013). Activation of the cellular unfolded protein response by recombinant adeno-associated virus vectors. *PLoS One*, *8*(1), e53845. https://doi.org/10.1371/journal.pone.0053845

Chen, S.-J., Johnston, J., Sandhu, A., Bish, L. T., Hovhannisyan, R., Jno-Charles, O., Sweeney, H. L., & Wilson, J. M. (2013). Enhancing the utility of adeno-associated virus gene transfer through inducible tissue-specific expression. *Human Gene Therapy Methods*, *24*(4), 270–278. https://doi.org/10.1089/hgtb.2012.129

Clark, K. R., Voulgaropoulou, F., Fraley, D. M., & Johnson, P. R. (1995). Cell lines for the production of recombinant adeno-associated virus. *Human Gene Therapy*, *6*(10), 1329–1341. https://doi.org/10.1089/hum.1995.6.10-1329

Clément, N., Knop, D. R., & Byrne, B. J. (2009). Large-scale adeno-associated viral vector production using a herpesvirus-based system enables manufacturing for clinical studies. *Human Gene Therapy*, *20*(8), 796–806. https://doi.org/10.1089/hum.2009.094

Elmore, Z. C., Patrick Havlik, L., Oh, D. K., Anderson, L., Daaboul, G., Devlin, G. W., Vincent, H. A., & Asokan, A. (2021). The membrane associated accessory protein is an adeno-associated viral egress factor. *Nature Communications*, *12*(1), 6239. https://doi.org/10.1038/s41467-021-26485-4

François, A., Bouzelha, M., Lecomte, E., Broucque, F., Penaud-Budloo, M., Adjali, O., Moullier, P., Blouin, V., & Ayuso, E. (2018). Accurate titration of infectious AAV particles requires measurement of biologically active vector genomes and suitable controls. *Molecular Therapy. Methods & Clinical Development*, *10*, 223–236. https://doi.org/10.1016/j.omtm.2018.07.004

Galibert, L., Jacob, A., Savy, A., Dickx, Y., Bonnin, D., Lecomte, C., Rivollet, L., Sanatine, P., Boutin Fontaine, M., Le Bec, C., & Merten, O.-W. (2021). Monobac system–A single baculovirus for the production of rAAV. *Microorganisms*, *9*(9), 1799. https://doi.org/10.3390/microorganisms9091799

Grimm, D., Kern, A., Pawlita, M., Ferrari, F. K., Samulski, R. J., & Kleinschmidt, J. A. (1999). Titration of AAV-2 particles via a novel capsid ELISA: Packaging of genomes can limit production of recombinant AAV-2. *Gene Therapy*, *6*(7), 1322–1330. https://doi.org/10.1038/sj.gt.3300946

Herzog, R. W., VandenDriessche, T., & Ozelo, M. C. (2023). First hemophilia B gene therapy approved: More than two decades in the making. *Molecular Therapy*, *31*(1), 1–2. https://doi.org/10.1016/j.ymthe.2022.12.001

Huang, M. M., & Hearing, P. (1989). The adenovirus early region 4 open reading frame 6/7 protein regulates the DNA binding activity of the cellular transcription factor, E2F, through a direct complex. *Genes & Development*, *3*(11), 1699–1710. https://doi.org/10.1101/gad.3.11.1699

Im, D. S., & Muzyczka, N. (1990). The AAV origin binding protein Rep68 is an ATP-dependent site-specific endonuclease with DNA helicase activity. *Cell*, *61*(3), 447–457. https://doi.org/10.1016/0092-8674(90)90526-k

Jennings, K., Miyamae, T., Traister, R., Marinov, A., Katakura, S., Sowders, D., Trapnell, B., Wilson, J. M., Gao, G., & Hirsch, R. (2005). Proteasome inhibition enhances AAV-mediated transgene expression in human synoviocytes in vitro and in vivo. *Molecular Therapy*, *11*(4), 600–607. https://doi.org/10.1016/j.ymthe.2004.10.020

King, J. A. (2001). DNA helicase-mediated packaging of adeno-associated virus type 2 genomes into preformed capsids. *The EMBO Journal*, *20*(12), 3282–3291. https://doi.org/10.1093/emboj/20.12.3282

Lee, Z., Lu, M., Irfanullah, E., Soukup, M., & Hu, W.-S. (2022). Construction of an rAAV producer cell line through synthetic biology. *ACS Synthetic Biology*, *11*, 3285–3295. https://doi.org/10.1021/acssynbio.2c00207

Lee, Z., Lu, M., Irfanullah, E., Soukup, M., Schmidt, D., & Hu, W. S. (2023). Development of an inducible, replication-competent assay cell line for titration of infectious recombinant adeno-associated virus vectors. *Human Gene Therapy*, *34*(3–4), 162–170. https://doi.org/10.1089/hum.2022.001.

Li, C., & Samulski, R. J. (2020). Engineering adeno-associated virus vectors for gene therapy. *Nature Reviews Genetics*, *21*, 255–272. https://doi.org/10.1038/s41576-019-0205-4

Lin, Y.-C., Boone, M., Meuris, L., Lemmens, I., Van Roy, N., Soete, A., Reumers, J., Moisse, M., Plaisance, S., Drmanac, R., Chen, J., Speleman, F., Lambrechts, D., Van de Peer, Y., Tavernier, J., & Callewaert, N. (2014). Genome dynamics of the human embryonic kidney 293 lineage in response to cell biology manipulations. *Nature Communications*, *5*(1), 4767. https://doi.org/10.1038/ncomms5767

Mainwaring, D., Joshi, A., Coronel, J., & Niehus, C. (2021). Transfer and scale-up from 10 L BioBLU® to Allegro™ STR 50 and STR 200 bioreactors. *Cell & Gene Therapy Insights*, *7*(4), 1347–1362. https://doi.org/10.18609/cgti.2021.178

Matsushita, T., Elliger, S., Elliger, C., Podsakoff, G., Villarreal, L., Kurtzman, G., Iwaki, Y., & Colosi, P. (1998). Adeno-associated virus vectors can be efficiently produced without helper virus. *Gene Therapy*, *5*(7), 938–945. https://doi.org/10.1038/sj.gt.3300680

Maurer, A. C., Pacouret, S., Cepeda Diaz, A. K., Blake, J., Andres-Mateos, E., & Vandenberghe, L. H. (2018). The assembly-activating protein promotes stability and interactions between AAV's viral proteins to nucleate capsid assembly. *Cell Reports*, *23*(6), 1817–1830. https://doi.org/10.1016/j.celrep.2018.04.026

Mendell, J. R., Al-Zaidy, S., Shell, R., Arnold, W. D., Rodino-Klapac, L. R., Prior, T. W., Lowes, L., Alfano, L., Berry, K., Church, K., Kissel, J. T., Nagendran, S., L'Italien, J., Sproule, D. M., Wells, C., Cardenas, J. A., Heitzer, M. D., Kaspar, A., Corcoran, S., … Kaspar, B. K. (2017). Single-dose gene-replacement therapy for spinal muscular atrophy. *New England Journal of Medicine*, *377*(18), 1713–1722. https://doi.org/10.1056/NEJMoa1706198

Merten, O. W., Gény-Fiamma, C., & Douar, A. M. (2005). Current issues in adeno-associated viral vector production. *Gene Therapy*, *12*(1), S51–S61. https://doi.org/10.1038/sj.gt.3302615

Mietzsch, M., Grasse, S., Zurawski, C., Weger, S., Bennett, A., Agbandje-McKenna, M., Muzyczka, N., Zolotukhin, S., & Heilbronn, R. (2014). OneBac: platform for scalable and high-titer production of adeno-associated virus serotype 1–12 vectors for gene therapy. *Human Gene Therapy*, *25*(3), 212–222. https://doi.org/10.1089/hum.2013.184

Mietzsch, M., Hering, H., Hammer, E.-M., Agbandje-McKenna, M., Zolotukhin, S., & Heilbronn, R. (2017). OneBac 2.0: Sf9 cell lines for production of AAV1, AAV2, and AAV8 vectors with minimal encapsidation of foreign DNA. *Human Gene Therapy Methods*, *28*(1), 15–22. https://doi.org/10.1089/hgtb.2016.164

Mietzsch, M., Smith, J. K., Yu, J. C., Banala, V., Emmanuel, S. N., Jose, A., Chipman, P., Bhattacharya, N., McKenna, R., & Agbandje-McKenna, M. (2020). Characterization of AAV-specific affinity ligands: Consequences for vector purification and development strategies. *Molecular Therapy - Methods & Clinical Development*, *19*, 362–373. https://doi.org/10.1016/j.omtm.2020.10.001

Mitchell, A. M., & Samulski, R. J. (2013). Mechanistic insights into the enhancement of adeno-associated virus transduction by proteasome inhibitors. *Journal of Virology*, *87*(23), 13035–13041. https://doi.org/10.1128/JVI.01826-13

Mohiuddin, I., Loiler, S., Zolotukhin, I., Byrne, B. J., Flotte, T. R., & Snyder, R. O. (2005). Herpesvirus-based infectious titering of recombinant adeno-associated viral vectors. *Molecular Therapy*, *11*(2), 320–326. https://doi.org/10.1016/j.ymthe.2004.08.030

Moreno, F., Lip, F., Rojas, H., & Anggakusuma, K. (2022). Development of an insect cell-based adeno-associated virus packaging cell line employing advanced Rep gene expression control system. *Molecular Therapy. Methods & Clinical Development*, *27*, 391–403. https://doi.org/10.1016/j.omtm.2022.10.015

Ogden, P. J., Kelsic, E. D., Sinai, S., & Church, G. M. (2019). Comprehensive AAV capsid fitness landscape reveals a viral gene and enables machine-guided design. *Science*, *366*(6469), 1139–1143. https://doi.org/10.1126/science.aaw2900

Penaud-Budloo, M., François, A., Clément, N., & Ayuso, E. (2018). Pharmacology of recombinant adeno-associated virus production. *Molecular Therapy - Methods & Clinical Development*, *8*, 166–180. https://doi.org/10.1016/j.omtm.2018.01.002

Prasad, V., & Greber, U. F. (2021). The endoplasmic reticulum unfolded protein response – Homeostasis, cell death and evolution in virus infections. *FEMS Microbiology Reviews*, *45*(5), fuab016. https://doi.org/10.1093/femsre/fuab016

Qiao, C., Li, J., Skold, A., Zhang, X., & Xiao, X. (2002). Feasibility of generating adeno-associated virus packaging cell lines containing inducible adenovirus helper genes. *Journal of Virology*, *76*(4), 1904–1913. https://doi.org/10.1128/jvi.76.4.1904-1913.2002

Querido, E., Blanchette, P., Yan, Q., Kamura, T., Morrison, M., Boivin, D., Kaelin, W. G., Conaway, R. C., Conaway, J. W., & Branton, P. E. (2001). Degradation of p53 by adenovirus E4orf6 and E1B55K proteins occurs via a novel mechanism involving a Cullin-containing complex. *Genes & Development*, *15*(23), 3104–3117. https://doi.org/10.1101/gad.926401

Rumachik, N. G., Malaker, S. A., Poweleit, N., Maynard, L. H., Adams, C. M., Leib, R. D., Cirolia, G., Thomas, D., Stamnes, S., Holt, K., Sinn, P., May, A. P., & Paulk, N. K. (2020). Methods matter: Standard production platforms for recombinant AAV produce chemically and functionally distinct vectors. *Molecular Therapy - Methods & Clinical Development*, *18*, 98–118. https://doi.org/10.1016/j.omtm.2020.05.018

Samulski, R. J., & Muzyczka, N. (2014). AAV-mediated gene therapy for research and therapeutic purposes. *Annual Review of Virology*, *1*(1), 427–451. https://doi.org/10.1146/annurev-virology-031413-085355

Schmidt, M., Afione, S., & Kotin, R. M. (2000). Adeno-associated virus type 2 Rep78 induces apoptosis through caspase activation independently of p53. *Journal of Virology*, *74*(20), 9441–9450. https://doi.org/10.1128/JVI.74.20.9441-9450.2000

Schwartz, R. A., Palacios, J. A., Cassell, G. D., Adam, S., Giacca, M., & Weitzman, M. D. (2007). The Mre11/Rad50/Nbs1 complex limits adeno-associated virus transduction and replication. *Journal of Virology*, *81*(23), 12936–12945. https://doi.org/10.1128/JVI.01523-07

Smith, R. H., Levy, J. R., & Kotin, R. M. (2009). A simplified baculovirus-AAV expression vector system coupled with one-step affinity purification yields high-titer rAAV stocks from insect cells. *Molecular Therapy*, *17*(11), 1888–1896. https://doi.org/10.1038/mt.2009.128

Sonntag, F., Schmidt, K., & Kleinschmidt, J. A. (2010a). A viral assembly factor promotes AAV2 capsid formation in the nucleolus. *Proceedings of the National Academy of Sciences*, *107*(22), 10220–10225. https://doi.org/10.1073/pnas.1001673107

Sonntag, F., Schmidt, K., & Kleinschmidt, J. A. (2010b). A viral assembly factor promotes AAV2 capsid formation in the nucleolus. *Proceedings of the National Academy of Sciences of the United States of America*, *107*(22), 10220–10225. https://doi.org/10.1073/pnas.1001673107

Soriano, A. M., Crisostomo, L., Mendez, M., Graves, D., Frost, J. R., Olanubi, O., Whyte, P. F., Hearing, P., & Pelka, P. (2019). Adenovirus 5 E1A interacts with E4orf3 to regulate viral chromatin organization. *Journal of Virology*, *93*(10), e00157–00119. https://doi.org/10.1128/JVI.00157-19

Srivastava, A., Lusby, E. W., & Berns, K. I. (1983). Nucleotide sequence and organization of the adeno-associated virus 2 genome. *Journal of Virology*, *45*(2), 555–564. https://doi.org/10.1128/jvi.45.2.555-564.1983

Srivastava, A., Mallela, K. M. G., Deorkar, N., & Brophy, G. (2021). Manufacturing challenges and rational formulation development for AAV viral vectors. *Journal of Pharmaceutical Sciences*, *110*(7), 2609–2624. https://doi.org/10.1016/j.xphs.2021.03.024

Strobel, B., Klauser, B., Hartig, J. S., Lamla, T., Gantner, F., & Kreuz, S. (2015). Riboswitch-mediated attenuation of transgene cytotoxicity increases adeno-associated virus vector yields in HEK-293 cells. *Molecular Therapy*, *23*(10), 1582–1591. https://doi.org/10.1038/mt.2015.123

Stutika, C., Gogol-Döring, A., Botschen, L., Mietzsch, M., Weger, S., Feldkamp, M., Chen, W., & Heilbronn, R. (2016). A comprehensive RNA sequencing analysis of the adeno-associated virus (AAV) type 2 transcriptome reveals novel AAV transcripts, splice variants, and derived proteins. *Journal of Virology*, *90*(3), 1278–1289. https://doi.org/10.1128/JVI.02750-15

Su, W., Patrício, M. I., Duffy, M. R., Krakowiak, J. M., Seymour, L. W., & Cawood, R. (2022). Self-attenuating adenovirus enables production of recombinant adeno-associated virus for high manufacturing yield without contamination. *Nature Communications*, *13*(1), 1182. https://doi.org/10.1038/s41467-022-28738-2.

Subramanian, S., Maurer, A. C., Bator, C. M., Makhov, A. M., Conway, J. F., Turner, K. B., Marden, J. H., Vandenberghe, L. H., & Hafenstein, S. L. (2019). Filling adeno-associated virus capsids: Estimating success by Cryo-electron microscopy. *Human Gene Therapy*, *30*(12), 1449–1460. https://doi.org/10.1089/hum.2019.041

Tenenbaum, L., Chtarto, A., Lehtonen, E., Velu, T., Brotchi, J., & Levivier, M. (2004). Recombinant AAV-mediated gene delivery to the central nervous system. *The Journal of Gene Medicine*, *6*(S1), S212–S222. https://doi.org/10.1002/jgm.506

Trempe, J. P., & Carter, B. J. (1988). Regulation of adeno-associated virus gene expression in 293 cells: Control of mRNA abundance and translation. *Journal of Virology*, *62*(1), 68–74. https://doi.org/10.1128/jvi.62.1.68-74.1988

Urabe, M., Ding, C., & Kotin, R. M. (2002). Insect cells as a factory to produce adeno-associated virus type 2 vectors. *Human Gene Therapy*, *13*(16), 1935–1943. https://doi.org/10.1089/10430340260355347

Vachon, V. K., & Conn, G. L. (2016). Adenovirus VA RNA: An essential pro-viral non-coding RNA. *Virus Research*, *212*, 39–52. https://doi.org/10.1016/j.virusres.2015.06.018

Wang, B., Li, J., Fu, F. H., Chen, C., Zhu, X., Zhou, L., Jiang, X., & Xiao, X. (2008). Construction and analysis of compact muscle-specific promoters for AAV vectors. *Gene Therapy*, *15*(22), 1489–1499. https://doi.org/10.1038/gt.2008.104

Ward, P., Dean, F. B., O'Donnell, M. E., & Berns, K. I. (1998). Role of the adenovirus DNA-binding protein in in vitro adeno-associated virus DNA replication. *Journal of Virology*, *72*(1), 420–427. https://jvi.asm.org/content/jvi/72/1/420.full.pdf

Wright, J. (2014). Product-related impurities in clinical-grade recombinant AAV vectors: Characterization and risk assessment. *Biomedicines*, *2*(1), 80–97. https://doi.org/10.3390/biomedicines2010080

Wyborski, D. L., & Short, J. M. (1991). Analysis of inducers of the *E.coli* lac repressor system mammalian cells and whole animals. *Nucleic Acids Research*, *19*(17), 4647–4653. https://doi.org/10.1093/nar/19.17.4647

Zeltner, N., Kohlbrenner, E., Clément, N., Weber, T., & Linden, R. M. (2010). Near-perfect infectivity of wild-type AAV as benchmark for infectivity of recombinant AAV vectors. *Gene Therapy*, *17*(7), 872–879. https://doi.org/10.1038/gt.2010.27

SUPPORTING INFORMATION

Additional supporting information can be found online in the Supporting Information section at the end of this article.

How to cite this article: Lu, M., Lee, Z., Lin, Y.-C., Irfanullah, I., Cai, W., & Hu, W.-S. (2024). Enhancing the production of recombinant adeno-associated virus in synthetic cell lines through systematic characterization. *Biotechnology and Bioengineering*, *121*, 341–354. https://doi.org/10.1002/bit.28562